



## Short communication

# Electrospun nanofiber of hybrid manganese oxides for supercapacitor: Relevance to mixed inorganic interfaces



Eunhee Lee, Taemin Lee, Byeong-Su Kim\*

Interdisciplinary School of Green Energy and Department of Chemistry, Ulsan National Institute of Science and Technology (UNIST), Ulsan 689-798, Republic of Korea

## HIGHLIGHTS

- 3-Dimensional  $\text{MnO}_x$  nanofiber was formed by electrospinning.
- Upon calcination at different temperatures,  $\text{MnO}_x$  NFs became variable composition of  $\text{Mn}_3\text{O}_4$  to  $\text{Mn}_2\text{O}_3$ .
- This study examined the supercapacitor performance depending on the phases of  $\text{MnO}_x$ .
- We found that mixed phase exhibited a higher capacity than that of respective single phase.
- The high specific capacitance was attributed to 3D structure and the reduced interfacial resistance.

## ARTICLE INFO

## Article history:

Received 3 December 2013

Received in revised form

5 January 2014

Accepted 6 January 2014

Available online 15 January 2014

## Keywords:

Electrospun nanofiber

Manganese oxides

Mixed phase

Supercapacitor

Three-dimensional (3D) electrode

## ABSTRACT

We prepare electrospun nanofibers (NFs) from a poly(N-vinylpyrrolidone)/manganese (II) acetate composite by electrospinning for application in supercapacitors. As-spun hybrid NFs are calcined at different temperatures to remove the polymer matrix, resulting in inorganic  $\text{MnO}_x$  NFs of variable compositional ratios of  $\text{Mn}_3\text{O}_4$  to  $\text{Mn}_2\text{O}_3$ . Interestingly, the sample of  $\text{MnO}_x$  NFs that is calcined at 500 °C exhibits the highest electrochemical performance, reaching a high specific capacitance of 360.7  $\text{F g}^{-1}$  at a current density of 1  $\text{A g}^{-1}$ . This remarkable performance is attributed to the unique three-dimensional morphology and the reduced interfacial resistance of the mixed-phase  $\text{MnO}_x$  NFs within the matrix electrode and the electrolyte.

© 2014 Elsevier B.V. All rights reserved.

## 1. Introduction

Due to the exhaustion of natural resources and associated environmental issues as well as the increasing demand of energy for future portable devices and electric vehicles, there has been an intense interest in alternative energy conversion and storage systems with high efficiency, low cost, and environmental benignity [1–3]. Among many energy storage devices, electrochemical capacitors, also known as supercapacitors, have attracted considerable attention because of their high power density, fast charge–discharge rate, long cycle life, wide thermal operating range, and low maintenance cost. Therefore, the performance of electrochemical capacitors is complementary to those of secondary batteries and fuel cells [4–6].

Supercapacitors are generally classified into two types depending on their charge storage mechanism and the active materials used. Electric double-layer capacitors store electrical charges at the interface of a porous, carbon-based electrode and an electrolyte based on the non-Faradaic reaction [4,7,8]. On the other hand, pseudocapacitors utilize the Faradaic reaction of redox-active materials such as conducting polymers and metal oxides [4,9–11]. In particular, transition metal oxides that exhibit pseudocapacitive behavior, such as  $\text{RuO}_2$  [12–14],  $\text{MnO}_x$ ,  $\text{NiO}$  [15,16],  $\text{CoO}$  [17], and  $\text{Fe}_3\text{O}_4$  [18], have been proposed as promising electrode materials for supercapacitors because of their high capacitance and good cycling stability. Among the above oxides, manganese oxide ( $\text{MnO}_x$ ) is clearly noteworthy, displaying fine specific capacitance (200–600  $\text{F g}^{-1}$ ) and reversible charge–discharge feature with its natural abundance and low cost [6,19–22]. Despite these favorable features of  $\text{MnO}_x$ , its poor electric conductivity and stability often cause unsatisfactory performance in supercapacitors. In addition, various oxidation states of  $\text{MnO}_x$  result in a range of different crystalline

\* Corresponding author. Tel.: +82 52 217 2923; fax: +82 52 217 2019.  
E-mail addresses: [bskim19@gmail.com](mailto:bskim19@gmail.com), [bskim19@unist.ac.kr](mailto:bskim19@unist.ac.kr) (B.-S. Kim).

phases with potentially different electrochemical behaviors. However, the relationship between phase structure and electrochemical properties of  $\text{MnO}_x$  has not been fully studied.

In order to improve supercapacitor performance, several approaches have been proposed, including developing new materials by deposition of electroactive metallic nanoparticles and conducting polymers, and creating new electrode structures [4,22–24]. As a representative approach, three-dimensional (3D), porous electrodes are known to exhibit superior capacitance because of increased specific surface area and enhanced access of electrolytes to the surface of the electrodes. In this regard, electrospinning can form porous, 3D electrodes from continuous, 1D nanofibers (NFs) of various materials [25–28]. Furthermore, electrospinning not only fabricates polymer and inorganic fibers with various dimensions, but also produces unique fiber structures such as hollow, core–shell, or porous structure [29–31].

In this report, we describe the fabrication of porous, 3D electrodes composed of  $\text{MnO}_x$  NFs by electrospinning for application in supercapacitors (Scheme 1). Specifically, a polymer matrix of poly(*N*-vinylpyrrolidone) (PVP) mixed with manganese (II) acetate ( $\text{Mn}(\text{CH}_3\text{COO})_2$  or  $\text{Mn}(\text{OAc})_2$ ) was employed to form continuous, 3D NFs of controlled dimensions. Upon calcination at different temperatures (400, 500, 600, and 700 °C), these NFs were transformed into hybrid  $\text{MnO}_x$  NFs with a varying degree of mixed phase of  $\text{Mn}_3\text{O}_4$  and  $\text{Mn}_2\text{O}_3$  in varying ratios. Interestingly, the relative composition of each phase was demonstrated to have a considerable influence on the supercapacitor performance by a series of electrochemical characterization measurements. For example, we confirmed that a mixed phase of  $\text{Mn}_2\text{O}_3$  and  $\text{Mn}_3\text{O}_4$  delivered a higher capacitance ( $360.7 \text{ F g}^{-1}$ ) than either of its individual material oxide taken individually, arising from the unique 3D morphology and the reduced interfacial resistance of the mixed phase within the matrix electrode and the electrolyte.

## 2. Experimental

### 2.1. Preparation of electrospun $\text{MnO}_x$ NFs

Poly(*N*-vinyl pyrrolidone) (PVP) solution was prepared by dissolving PVP powder ( $M_w$  1,300,000  $\text{g mol}^{-1}$ ) in deionized water (20 wt%). Then,  $\text{Mn}(\text{OAc})_2/\text{PVP}$  solution was prepared by dissolving manganese acetate (20 wt%) in PVP solution. This solution was stirred for at least one day in order to obtain homogeneously distributed solutions. The solution obtained was injected from a syringe and syringe was fixed in syringe pump. The size of the needle in the electrospinning was 25 G, and the needle was

connected to high-voltage power supply. The flow rate of the syringe pump was fixed at  $10 \mu\text{l min}^{-1}$ , and the distance between the needle and collector was 10 cm and the applied voltage was 25 kV. The electrospun  $\text{Mn}(\text{OAc})_2/\text{PVP}$  NFs were annealed at different temperatures (400, 500, 600 and 700 °C) to remove the polymer matrix and result in the  $\text{MnO}_x$  NFs.

### 2.2. Structural characterizations

The morphology and fiber diameter of the prepared  $\text{MnO}_x$  NFs were investigated using a field emission scanning electron microscopy (FESEM, FEI, Nanonova 230) and transmission electron microscopy (TEM, JEOL JEM-2100 accelerating voltage of 200 kV, Gatan CCD camera). X-ray diffraction (XRD) measurements were employed by a high-power X-ray diffractometer (Rigaku Co., D/MAZX 2500V/PC) from  $10^\circ$  to  $80^\circ$ .

### 2.3. Electrochemical characterization

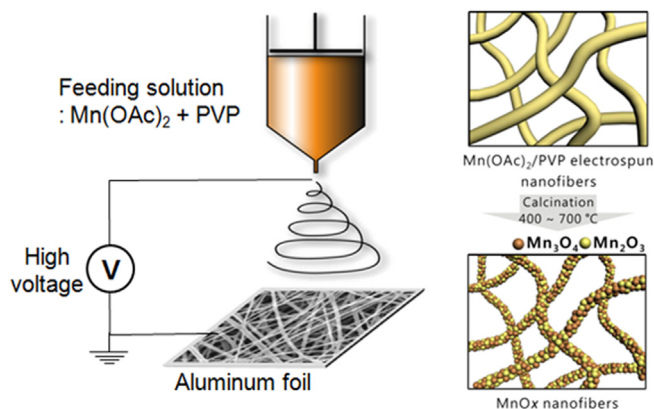
Electrochemical performance of the electrospun  $\text{MnO}_x$  NFs were carried out with a standard three-electrode test cell with 0.5 M  $\text{Na}_2\text{SO}_4$  aqueous solution as electrolyte. Platinum wire and  $\text{Ag}/\text{AgCl}$  were used as a counter and reference electrode, respectively. The characterization of the electrochemical performance for the  $\text{MnO}_x$  electrode was conducted using a VMP3 electrochemical potentiostat (BioLogic Inc.). Cyclic voltammograms (CVs) and the galvanostatic charge–discharge test were carried out with a potential window from  $-0.2$  to  $0.8 \text{ V}$  versus  $\text{Ag}/\text{AgCl}$  in 0.50 M  $\text{Na}_2\text{SO}_4$  electrolyte with scan rates from 5 to  $200 \text{ mV s}^{-1}$  and a current density of  $1 \text{ A g}^{-1}$ . In order to internal resistance of  $\text{MnO}_x$  electrode, measurement of electrochemical impedance was performed in frequency range of 100 kHz–100 MHz.

## 3. Results and discussion

### 3.1. Characterization of electrospun $\text{MnO}_x$ NFs

Initially,  $\text{Mn}(\text{OAc})_2/\text{PVP}$  NFs were successfully fabricated by electrospinning using the procedures outlined in the experimental section. Fig. 1 shows the SEM images and diameter distribution of the as-spun  $\text{Mn}(\text{OAc})_2/\text{PVP}$  NFs and the  $\text{MnO}_x$  NFs formed after calcination at temperatures from 400 to 700 °C. As shown in Fig. 1a, as-spun  $\text{Mn}(\text{OAc})_2/\text{PVP}$  NFs were randomly oriented in a continuous, 3D, porous internal structure. The range of NF diameters in the sample was relatively narrow, and no beads were formed. The polymeric component (PVP) was completely degraded at  $\sim 400$  °C in air, as determined by thermogravimetric analysis (TGA). Accordingly, the as-spun  $\text{Mn}(\text{OAc})_2/\text{PVP}$  NFs were calcined above 400 °C in air (Fig. S1 in Supporting information). After calcination at different temperatures, the 3D porous structure was retained without significant structural deformation. However, the diameter of  $\text{MnO}_x$  NFs decreased after calcination due to the removal of the PVP matrix and the crystallization of  $\text{MnO}_x$ ; for example, the average diameter of as-spun fiber decreased from  $135 \pm 18 \text{ nm}$  to  $72.3 \pm 14.3 \text{ nm}$  (400 °C),  $64.2 \pm 12.6 \text{ nm}$  (500 °C),  $52.7 \pm 8.9 \text{ nm}$  (600 °C) and  $54.5 \pm 6.9 \text{ nm}$  (700 °C), respectively.

Various forms of manganese oxide such as  $\alpha$ - $\text{MnO}_2$ ,  $\delta$ - $\text{MnO}_2$ ,  $\lambda$ - $\text{MnO}_2$ ,  $\text{Mn}_2\text{O}_3$ , and  $\text{Mn}_3\text{O}_4$  are known to exist depending on the conditions of annealing [32]. We further characterized the phase composition of  $\text{MnO}_x$  NFs after calcination by X-ray diffraction (XRD) (Fig. 2). The XRD patterns of  $\text{MnO}_x$  fibers calcined at different temperatures corresponded to either  $\text{Mn}_3\text{O}_4$  (JCPDS 024-0734) or  $\text{Mn}_2\text{O}_3$  (JCPDS 073-1826), or a combination of both. The NFs calcined at 400 °C adopted the tetragonal  $\text{Mn}_3\text{O}_4$  phase exclusively (Fig. 2a). Above 400 °C,  $\text{Mn}_3\text{O}_4$  transformed into the more oxidized



**Scheme 1.** Schematic representation for the fabrication of the electrospun fiber and subsequent calcination process for hybrid  $\text{MnO}_x$  NF supercapacitors.

Download English Version:

<https://daneshyari.com/en/article/1284231>

Download Persian Version:

<https://daneshyari.com/article/1284231>

[Daneshyari.com](https://daneshyari.com)